◆ Human Brain Mapping 38:5292–5306 (2017) ◆

Analysis of Structure–Function Network Decoupling in the Brain Systems of Spastic Diplegic Cerebral Palsy

Dongha Lee,[1,2] Chongwon Pae,[2,3] Jong Doo Lee,[4] Eun Sook Park,[5] Sung-Rae Cho,[5] Min-Hee Um,[2] Seung-Koo Lee,[6] Maeng-Keun Oh,[3] and Hae-Jeong Park [2,3,6,7,8]*

[1]*Faculty of Psychology and Education Sciences, University of Coimbra, Coimbra, Portugal*
[2]*BK21 PLUS Project for Medical Science, Korea*
[3]*Department of Nuclear Medicine, Yonsei University College of Medicine, Seoul, Republic of Korea*
[4]*Department of Radiology and Nuclear Medicine, International St. Mary's Hospital, Catholic Kwandong University College of Medicine, Incheon, South Korea*
[5]*Department of Rehabilitation Medicine, Yonsei University College of Medicine, Seoul, Republic of Korea*
[6]*Department of Radiology, Yonsei University College of Medicine, Seoul, Republic of Korea*
[7]*Department of Cognitive Science, Yonsei University, Seoul, Republic of Korea*
[8]*Center for Systems and Translational Brain Sciences, Institute of Human Complexity and Systems Science, Yonsei University, Seoul, Republic of Korea*

Abstract: Manifestation of the functionalities from the structural brain network is becoming increasingly important to understand a brain disease. With the aim of investigating the differential structure–function couplings according to network systems, we investigated the structural and functional brain networks of patients with spastic diplegic cerebral palsy with periventricular leukomalacia compared to healthy controls. The structural and functional networks of the whole brain and motor system, constructed using deterministic and probabilistic tractography of diffusion tensor magnetic resonance images and Pearson and partial correlation analyses of resting-state functional magnetic resonance images, showed differential embedding of functional networks in the structural networks in patients. In the whole-brain network of patients, significantly reduced global network efficiency compared to healthy controls were found in the structural networks but not in the functional networks, resulting in reduced structural–functional coupling. On the contrary, the motor network of patients had a significantly lower functional network efficiency over the intact structural network and a lower structure–function coupling than the control group. This reduced coupling but reverse directionality in the whole-brain and motor networks of patients was prominent particularly between the probabilistic structural and partial correlation-based functional networks. Intact (or less deficient) functional network over impaired structural networks of the whole brain and highly impaired functional network topology over the intact structural motor network might

Contract grant sponsor: National Research Foundation of Korea (NRF); Contract grant number: 2014R1A2A1A10052762.

*Correspondence to: Hae-Jeong Park, PhD; Department of Nuclear Medicine, Yonsei University College of Medicine, 50 Yonsei-ro, Sinchon-dong, Seodaemun-gu, Seoul 120-752, Republic of Korea. E-mail: parkhj@yonsei.ac.kr

Received for publication 10 March 2017; Revised 8 July 2017; Accepted 13 July 2017.

DOI: 10.1002/hbm.23738
Published online 21 July 2017 in Wiley Online Library (wileyonlinelibrary.com).

subserve relatively preserved cognitions and impaired motor functions in cerebral palsy. This study suggests that the structure–function relationship, evaluated specifically using sparse functional connectivity, may reveal important clues to functional reorganization in cerebral palsy. *Hum Brain Mapp 38:5292–5306, 2017*.

Key words: cerebral palsy; structure–function relationship; brain network; functional reorganization

INTRODUCTION

The relationship between structure and function has recently been framed in terms of networks and is receiving growing attention not only in exploring organizational principles of the brain [Deco et al., 2011] but also in understanding brain diseases, for example, structural–functional network couplings in schizophrenia [Cocchi et al., 2014; van den Heuvel et al., 2013] and amyotrophic lateral sclerosis [Schmidt et al., 2014]. The importance of this network approach to structure–function relationship is not only in its ability to describe the abnormal reorganization of the functional network over the structural network but also in its ability to explain intact (or less deficient) information exchange among brain regions even after anatomical malformation or damage [Bullmore and Sporns, 2009]. Recent researches on the structural and functional networks were promoted by the introduction of in vivo neuroimaging methods for brain connectivity, including diffusion tensor imaging (DTI) for structural networks and resting-state functional magnetic resonance imaging (rs-fMRI) for functional networks (see Park and Friston [2013] for review).

Using neuroimaging methods, we aimed to investigate the structure–function relationships in the brains of patients with cerebral palsy (CP), a broad range of diseases with nonprogressive permanent motor impairments. The cause of CP is multifactorial, including prenatal hypoxic ischemic injury, asphyxia, infections/inflammation, coagulopathies, and inheritance [Keogh and Badawi, 2006; Msall, 2004], which are often associated with cystic or diffuse periventricular leukomalacia (PVL) as a high risk factor for CP. Out of the various subtypes of CP, this study focuses on spastic diplegic cerebral palsy (SDCP) with PVL.

It has been shown that structural alterations in patients with CP and PVL are not confined to a PVL zone or motor-related pathways [Arzoumanian et al., 2003; Ceschin et al., 2015; Englander et al., 2013; Lee et al., 2011b; Nagae et al., 2007; Scheck et al., 2012; Thomas et al., 2005], but are rather widespread across the whole-brain white matter. Lee et al. [2011b] showed that patients with SDCP who were born prematurely had low diffusion anisotropy across the whole brain, as was found in adolescents with very low birth weights [Skranes et al., 2007] and in preterm children with CP [Ceschin et al., 2015].

However, the effects that these widespread structural alterations have on information transfer across the whole brain were rarely explored. Ceschin et al. [2015] showed reduced global efficiency of structural networks constructed using DTI in preterm children with CP. Diffuse reduction of structural connectivity across the whole brain was reported in severe compared to mild CP [Englander et al., 2013]. Despite not being a network analysis, several functional connectivity studies using resting state fMRI have revealed lower functional connectivity in patients with CP, especially in the sensorimotor regions [Burton et al., 2009; Lee et al., 2011b; Papadelis et al., 2014; Park et al., 2013b]. As these studies were performed using independent structural and functional network analyses, they provided a limited understanding of the divergence of functional networks from structural networks.

In this study, we explored the divergence of structural–functional networks of the whole brain and the motor network of SDCP with PVL. The motor network in this study was composed of the sensory-motor cortex, basal ganglia, and the thalamic circuits, which are considered to be primary centers of motor dysfunction, a major symptom of CP [Bottcher, 2010; Burton et al., 2009; Englander et al., 2013; Lee et al., 2011b; Msall, 2006; Park et al., 2013b; Thomas et al., 2005]. We evaluated structural and functional networks of patients and healthy controls using graph theoretical measures, and subsequently examined coupling between the two networks.

Despite widespread structural alterations, the cognitive impairment in CP is relatively less prevalent (23–44%) [Odding et al., 2006] and less prominent compared to the motor deficits. Therefore, we hypothesized that the whole-brain functional networks responsible for diverse cognitive functions in CP undergo reorganization under the global structural network abnormality, and that this would be reflected in an increased deviation from the structural networks. In contrast to relatively intact general cognitive functions, patients with CP show typical behavioral deficits in motor function. Accordingly, we expected that the motor network would exhibit a distinctive pattern of structural–functional network decoupling different from that of the whole brain network. To test the motor-system specificity in the structural–functional decoupling, we evaluated two visual systems that were segregated into the dorsal and ventral streams, the "what" and "where" systems [Goodale et al., 1982; Goodale and Milner, 1992; Milner and Goodale, 2006; Wang et al., 1999]. These visual systems were chosen as reference points because they are at the similar level within the cognitive hierarchy with the motor system and are relatively well understood than other cognitive networks.

TABLE I. Demographic data of patients with cerebral palsy

ID	Sex	Age	MRI diagnosis	Birth weight	Delivery (month)	GMFCS	Results	Remarks	Cognitive diagnosis
CP1	F	23	PVL	1.3	32	5	MMSE 29	MQ 112	Normal
CP2	F	8	PVL	0.8	27	1	FSIQ 102	VIQ 122, PIQ 79	Normal
CP3	M	22	PVL	1.7	32	1	FIM SC 7		Normal
CP4	M	13	PVL	1.97	32	5	FIM SC 7	Memory 6	Normal
CP5	M	20	PVL	1.4	32	1		ADL independent	Normal
CP6	M	15	PVL	1.5	32	1	FIM SC 6	Comprehension 6	Mild decreases
CP7	F	14	PVL	2	34	2	FSIQ 101	VIQ 122, PIQ 77, FIM SC 7	Normal
CP8	M	12	PVL	1.4	29	1	FIM SC 7		Normal
CP9	F	16	PVL	1.3	26	1	FSIQ 70	VIQ 93, PIQ 51, FIM SC 7	Normal
CP10	F	11	PVL	2.8	37	3	FIM SC 6–7	Memory 6	Mild decreases
CP11	M	9	PVL	2	33	1	FSIQ 55	VIQ 79, PIQ 51	Mild decreases
CP12	F	12	PVL	1.58	32	1		High rank at a public school	Normal
CP13	F	12	PVL	1.6	32	1	FSIQ 82	VIQ 105, PIQ 61	Normal
CP14	M	29	PVL	2.5	28	1	FIM SC 7		Normal

CP, cerebral palsy; F, female; M, male; PVL, periventricular leukomalacia; GMFCS, Gross Motor Function Classification System; MMSE, Mini Mental Status Examination; FIM, functional independence measure; ADL, activities of daily living; SC, social cognition; MQ, memory quotient; VIQ, verbal intelligence quotient; PIQ, performance intelligence quotient; FSIQ, full-scale intelligence quotient.

Technically, structural and functional brain networks have been defined in two different ways: dense networks and sparse networks. Probabilistic and deterministic tractography of diffusion weighted images construct dense and sparse structural networks, respectively. Probabilistic tractography has more power to reduce missing fibers and thus makes a denser network compared to deterministic tractography (which reconstructs a single streamline from a starting point). In constructing functional brain networks, functional connectivity has mostly been defined using Pearson correlation between the signals at two brain regions. As functional connectivity measured by Pearson correlation includes indirect interactions between two regions through a polysynaptic connection or a common modulation, it generates a denser functional network than a real functional interaction. Meanwhile, partial correlation analysis reduces these indirect connections and thus generates sparser functional networks. Till date, these definitions were independently used in previous whole-brain network studies and the relationship between the different types of structural and functional networks has seldom been investigated.

In this study, we focused on the structure–function coupling of CP with respect to probabilistic tractography and partial correlation analysis due to the representational power of structural connectivity and direct functional connectivity.

MATERIALS AND METHODS

Subjects

For this study, we used neuroimaging data from 14 patients with spastic diplegic CP (7 men and 7 women, age 8–29 years, mean age 14.7 years) and 20 healthy control subjects without neurological disorders (12 men and 8 women, age 7–29 years, mean age 14.5 years) enrolled in previous studies [Lee et al., 2011b]. The control group was age- and sex-matched without neurological and psychiatric disorders. All patients had PVL (end-stage), mainly diffuse periventricular white matter injury, according to the MRI-based diagnostic criteria: enlargement of the ventricles with irregular margins of the bodies and trigones of the lateral ventricles, loss of periventricular white matter, increased T2 signal, and thinning of the corpus callosum.

None of the patients had any significant cortical damage based on visual analysis. They were born prematurely (age < 38 weeks, range 26–37 weeks, mean 31.29 ± 2.9 weeks) with a low birth weight (range 0.8–2.8 kg, mean 1.7 ± 0.7 kg). All subjects received orthopedic surgery, such as heel cord lengthening to reduce spasticity, 3–58 months prior to MRI scanning. To evaluate the gross motor functions of children with cerebral palsy, we used the Gross Motor Function Classification System (GMFCS) level, which is a 5-level classification system; patients able to perform moderate movement (i.e., walking) were classified as GMFCS levels 1 and 2, those unable to walk without assistance as GMFCS levels 3 and 4, and those who had severe impairments that prevented movement as GMFCS level 5. GMFCS levels in the current patients were as follows: level 1, 10 subjects; level 2, 1 subject; level 3, 1 subject; and level 5, 2 subjects. Three of the 14 patients had mild cognitive impairment, while the rest were within the normal range according to one of clinical evaluations such as mini–mental state examination, full-scale intelligence quotient, and functional independence measure scale. The demographic data of the patients are summarized in Table I. This

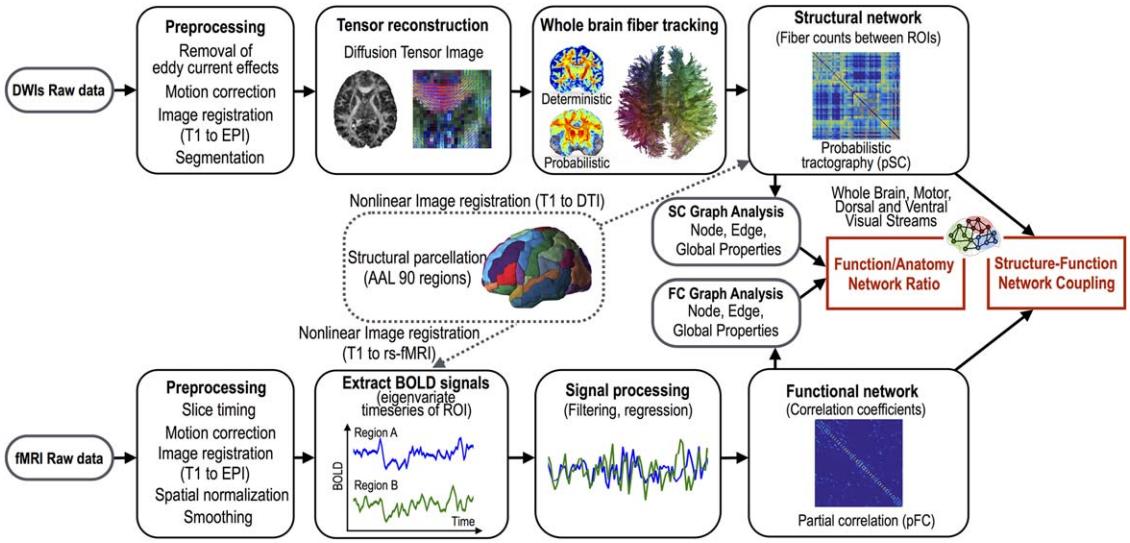

Figure 1.

Analyses of structure–function network couplings. Sparse and dense structural brain networks of individuals were constructed using the deterministic (SC) and probabilistic (pSC) fiber tractography of diffusion tensor image (DTI) among pairs of 90 cerebral regions. The connectivity matrix or structural network is defined with the number of estimated fibers between the ROIs. Dense and sparse functional networks were derived from Pearson (FC) and partial correlation analysis (pFC) of resting-state fMRI (rs-fMRI) time series at 90 regions after preprocessing. Graph-theoretic properties of the structural and functional networks and their functional-to-structural ratios were compared between patients with spastic diplegic cerebral palsy and healthy controls. Structural–functional network coupling was also evaluated between the groups. All structure–function relationship analyses in cerebral palsy and healthy controls were evaluated on the whole-brain, motor, and dorsal and ventral visual stream networks. [Color figure can be viewed at wileyonlinelibrary.com]

study was conducted in accordance with institutional guidelines based on the Code of Ethics of the World Medical Association (Declaration of Helsinki) and was approved by the Institutional Review Board of Severance Hospital.

Data Acquisition and Image Processing

All MRI data were acquired using a Philips 3.0-T scanner (Philips Intera; Philips Medical System, Best, The Netherlands) with an 8-channel SENSE head coil. All data were acquired using the same set of MRI protocols. High-resolution structural data were obtained from each subject using a three-dimensional T1-weighted MRI sequence (field of view, 220 mm; voxel size, $0.98 \times 0.98 \times 1.2$ mm^3; repetition time (TR), 3000 ms; echo time (TE), 125 ms).

Diffusion-weighted images were obtained using single-shot echo planar imaging (EPI) sequences from 45 noncollinear, noncoplanar diffusion-encoded gradient directions with the following parameters: 128×128 acquisition matrix; 220 mm field of view; 70 slices per volume; $1.72 \times 1.72 \times 2$ mm^3 voxels; TE, 60 ms; TR, 7.384 s; b factor, 600 s/mm^2; and no cardiac gating.

Resting-state fMRI data were acquired axially using T2*-weighted single-shot EPI using a 3.0 T Philips MRI scanner (Philips Systems, The Netherlands) with the following parameters: voxel size, $2.75 \times 2.75 \times 4.5$ mm^3; slice number, 31 (interleaved); matrix, 80×80; TR, 2000 ms; TE, 30 ms; and field of view, 220×220 mm^2 for 330 s (165 scans). During resting-state fMRI scanning, subjects were instructed to keep their eyes closed, without sleeping or specific thinking. After scanning, the subjects were asked to report their sleepiness and general condition. Foam pads were used to reduce head motion during all MRI scans.

Figure 1 summarizes all the procedures conducted in this study.

We first parcellated the cerebral brain based on the automated anatomical labeling (AAL) map [Tzourio-Mazoyer et al., 2002]. As some labels in the initial AAL map are not parcellated accurately enough to locate the cortical gray matter according to the cortical folding pattern, we modified the label map manually in the International Consortium for Brain Mapping (ICBM) template brain, which was used for the fMRI and DTI analysis in this study.

To define structural networks, we first defined 90 cerebral nodes in the individual diffusion tensor space. For this purpose, we co-registered T1-weighted images to DTI using a nonlinear registration algorithm between the T1-weighted images and the non-diffusion-weighted b0 images in DTI for each individual. The nonlinear co-registration algorithm

maximizes normalized mutual information between DTI and T1-weighted images resampled on second-order B-Spline basis functions. This co-registration was conducted after adjusting for eddy-current effects and removing motion artifacts [Nam and Park, 2011]. The modified AAL map in the MNI template space was transformed into the individual T1-weighted MRI by applying the inverse nonlinear transformation from individual T1-weighted MRI to the ICBM T1-weighted MRI using the DARTEL toolbox in SPM8 [Ashburner, 2007]. The label map in the individual T1 space was transformed to individual DTI space by applying co-registration from T1-weighted images to DTI as described above.

Preprocessing of fMRI data was conducted using statistical parametric mapping (SPM8, http://www.fil.ion.ucl.ac.uk/spm/) [Friston et al., 1995]. All EPI data underwent standard preprocessing steps, including correction of acquisition time delays between different slices, correction for head motion by realigning all consecutive volumes to the first image of the session, and co-registration of T1-weighted images to the first EPI data using the nonlinear registration algorithm described above. Co-registered T1-images were used to spatially normalize the functional EPI into MNI template space using nonlinear transformation in SPM8.

fMRI time series for 90 cerebral regions out of the modified AAL map were extracted from the normalized fMRI data in the MNI template space. Principal component analysis was applied to extract a representative time series for multiple voxels in each region. Time series of eigenvalues corresponding to the first eigenvector, that is, the mode was used as a representative activity for the region. After discarding the first five scans due to stability issues, we preprocessed the fMRI time series by regressing out effects of six rigid motions and their derivatives, three principal components of the white matter and the cerebrospinal fluid masks, linear repressors, quadratic repressors, and high-pass filtering with a cutoff frequency 0.009 Hz. The white matter and cerebrospinal fluid masks were segmented using individual T1 images.

End-stage PVL leads to enlargement of the ventricles due to loss of periventricular white matter. To determine the group-wise average location of PVL in this study, we conducted a statistical parametric mapping using the cerebrospinal fluid (CSF) probability maps of patients and healthy controls. The CSF probabilistic maps were generated by segmenting individual T1-weighted MRI in the template space (after spatial normalization) using SPM8. Subsequently, we conducted voxel-wise two-sample t tests for the CSF probability maps using SPM8.

Structural Network Construction: Probabilistic Tractography

To construct a probabilistic structural network (pSC), we conducted probabilistic tractography using FMRIB's diffusion toolbox (FDT v3.0, http://fsl.fmrib.ox.ac.uk/fsl/fslwiki/FDT). We performed "BedpostX" that samples propagation directions according to probabilistic orientation distribution at each voxel in the Bayesian framework using Markov Chain Monte Carlo sampling [Behrens et al., 2007]. Probabilistic fiber density was estimated using "ProbtrackX" with the following parameters: 5,000 samples within each voxel, 0.2 curvature threshold, 0.5mm step length, and 2,000 steps per sample. Using this probabilistic fiber tracking, a structural connectivity matrix for the motor network of each individual was constructed by counting the number of fibers that interconnected every pair of the 90 brain regions. We made the connectivity matrix symmetric by averaging bidirectional connectivity to evaluate structure–function couplings in this network.

Functional Network Construction: Partial Correlation Analysis

We used partial correlation (pFC) as a primary index for functional connectivity. The partial correlation matrix of the mode time series (eigenvalue time series of the first principal component of fMRI time series at each brain region) among the 90 regions was calculated using the graphical Least Absolute Shrinkage and Selection Operator (gLASSO) technique [Friedman et al., 2008]. As a gLASSO method, we used sparse inverse covariance estimation (SICE) [Huang et al., 2010]. The regularization parameter λ was determined using Stability Approach to Regularization Selection (StARS) [Liu et al., 2010]. As edges generally shrink after gLASSO, we adjusted the edges to reflect connectivity strength properly [Zou et al., 2015] using a sample covariance matrix and a sparse structure of original precision matrix [Dempster, 1972]. Functional networks were constructed by thresholding pFC with $r > 0$, as gLASSO shrinks unrelated interactions (edges) to zero.

Network Analysis and Structure–Functional Network Coupling Measures

We conducted graph theoretical network analysis to investigate the topological properties (i.e., local and global properties) of whole-brain networks in patients with CP and healthy controls. We also calculated network properties within the motor network, and the dorsal and ventral visual stream networks. The motor network was composed of 16 nodes, including the precentral gyrus, the supplementary motor area, the postcentral gyrus, the paracentral lobule, the caudate, the putamen, the pallidum, and the thalamus in both hemispheres based on previous studies [Kahan et al., 2014; Lee et al., 2011b; Park et al., 2013a; Taniwaki et al., 2003; Wei et al., 2014] (Fig. 2A). Two visual stream networks were defined according to previous literatures [Goodale et al., 1982; Goodale and Milner, 1992; Milner and Goodale, 2006; Wang et al., 1999] (Fig. 2A). The dorsal visual stream network consists of 20 brain regions—the bilateral superior/inferior parietal gyrus, the supramarginal gyrus, the angular

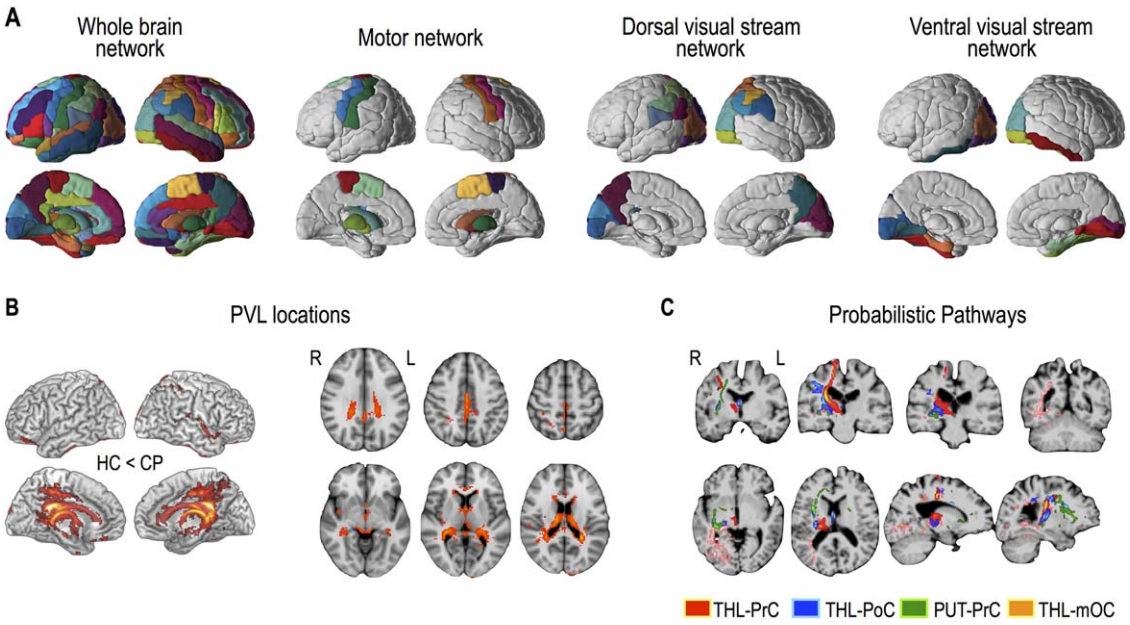

Figure 2.

Whole-brain network regions, subnetwork regions, periventricular leukomalacia (PVL) locations, and probabilistic structural pathways. Brain regions for the whole-brain network (modified AAL 90 regions), the motor network (16 regions), the dorsal visual pathway network (20 regions), and the ventral visual pathway network (16 regions) are displayed (A). Rendering and slice displays of increased cerebrospinal fluid (CSF) probability in cerebral palsy (CP) compared to healthy controls (HC) with a threshold at $P < 0.005$ and more than 73 continuous voxels were displayed as PVL locations (B). Examples of probabilistic maps of the structural connectivity for a patient (CP1) were overlaid on the T1-weighted image of the patient (C). The probabilistic pathways between the right thalamus (THL) and the right precentral gyrus (PrC) were colored in red, between the right thalamus and the right postcentral gyrus (PoC) in blue, between the right thalamus and the right middle occipital cortex (mOC) in pink, and between the right putamen (PUT) and the right precentral gyrus in green. R: right, L: left. [Color figure can be viewed at wileyonlinelibrary.com]

gyrus, the precuneus, the cuneus, the calcarine sulcus, and the superior/middle/inferior occipital gyrus. The bilateral fusiform gyrus, the lingual gyrus, the parahippocampus, the inferior temporal gyrus, the calcarine sulcus, and the superior/middle/inferior occipital gyrus were included for the ventral visual stream network (total 16 regions).

We calculated global properties (global node strength, global, and local efficiencies) and local properties (node strength, node efficiency, and betweenness centrality) using the BCT toolbox [Rubinov and Sporns, 2010] for structural and functional networks of whole-brain networks and three subnetworks.

The global and local network properties are explained in detail in Rubinov and Sporns [2010]. Briefly, node strength of a node is the sum of all connection weights between the node and the other nodes. Node efficiency of a node is defined as the mean of all pairs of shortest path lengths between the node and the other nodes. Global node strength is the average of all node strengths. Global efficiency [Latora and Marchiori, 2001] is the average of all node efficiencies. Local efficiency is the global efficiency calculated on node neighborhoods.

We defined the coupling between structural and functional networks for each subject using a correlation coefficient between strengths of the structural connections (numbers of fibers) and their functional counterparts. Considering the influences of negative correlations reported in Skudlarski et al. [2008], we correlated structural connectivity with positive functional connectivity after regarding the negative functional connectivity as zero. A correlation coefficient between structural and functional connectivity matrices in each individual was calculated after vectorizing both connectivity matrices. We evaluated the structural–functional couplings both in the whole-brain network and in the three subnetworks.

For each individual, we also evaluated the ratio of network properties (global efficiency, global strength, and local efficiency) of the functional and structural networks to examine directional changes in the functional network property, normalized by the structural network property. Since changes in functional couplings did not provide directionality in the (functional) information exchange, that is, whether this decoupling appears to increase or decrease the information exchange within each structural

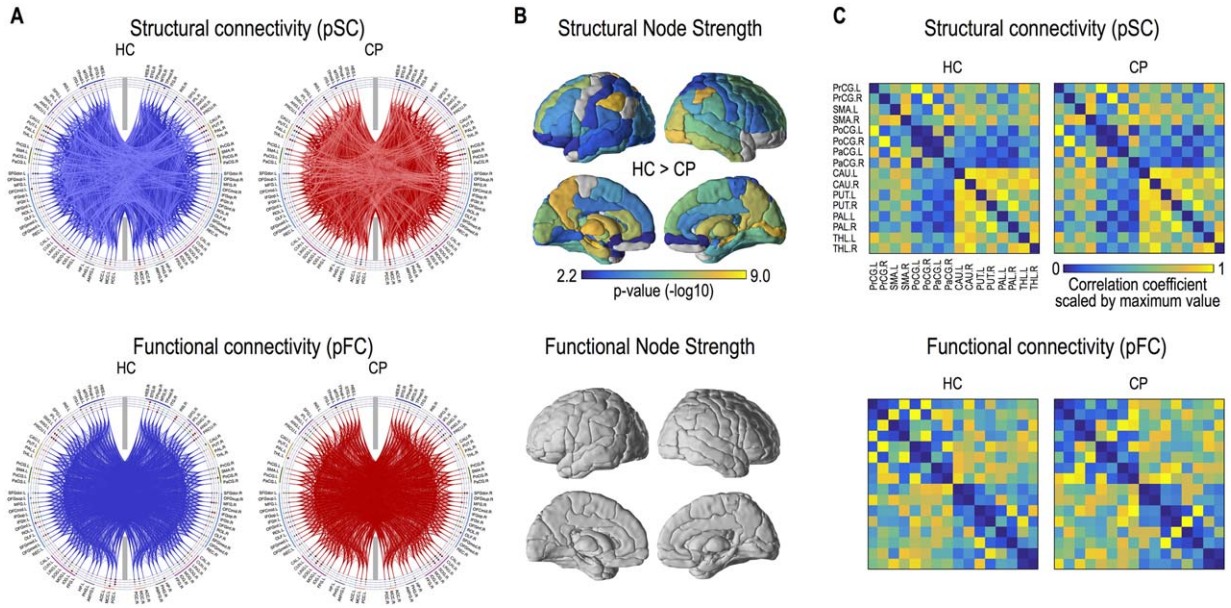

Figure 3.

Structural and functional networks in cerebral palsy (CP) and healthy controls (HC). Group-average structural and functional networks are presented in blue lines for HC and in red lines for patients with CP (A). Structural connectivity was evaluated using probabilistic tractography (pSC) and functional connectivity was derived using partial correlation analysis (pFC). Brain regions having significantly reduced node strength of the structural network in CP are displayed (FDR < 0.01) (B). Group adjacency matrices (connectivity matrices) of structural and functional motor networks are presented (C). [Color figure can be viewed at wileyonlinelibrary.com]

network system, this ratio index would be useful in clarifying this directionality in decoupling; greater values indicate increased efficiency in functional networks when normalized by structural efficiency while the reverse is true for smaller values.

Two-sample t tests were applied to evaluate all the measures. For the local node properties and edge degrees, statistical differences were considered to be significant if P values passed the threshold of false discovery rate (FDR) <0.05 to correct for multiple testing.

RESULTS

Structural and Functional Networks in Cerebral Palsy (CP) and Healthy Controls (HC)

Figure 2A displays the whole-brain network and three subnetworks (motor and dorsal and ventral visual stream networks) evaluated in this study. The group-wise average location of PVL in the current patient group is displayed in Figure 2B, which shows an enlarged CSF space (increased CSF probability map) in the medial and posterior part of the brain. Figure 2C displays examples of probabilistic maps of structural connectivity for a patient (CP1). The probabilistic pathways between the thalamus and the precentral gyrus, postcentral gyrus, and the middle occipital cortex, and between the putamen and the precentral gyrus were overlaid on the T1-weighted image of the patient.

The whole-brain networks of healthy controls and patients constituted by dense structural connectivity and sparse functional connectivity are displayed in Figure 3A. The statistical group differences in node strengths of structural and functional networks measured using probabilistic tractography and partial correlation analysis are summarized in Table II and Figure 3B. Significantly lower structural node strengths in patients with CP compared to healthy controls were widely distributed across the whole brain (Fig. 3B). However, there were no statistically significant differences in the node strengths between the sparse functional network groups (Fig. 3B and Table II).

The structural and functional connectivity maps in the motor network are presented in Figure 3C. Patients and healthy controls showed similar structural but different functional network patterns. The statistical group differences are summarized in Table II.

Global Efficiency of Structural and Functional Networks

Table II summarizes the statistical group-wise differences in the global properties of structural and functional

TABLE II. Global network properties, ratios, and couplings of dense structural and sparse functional networks

	Dense structural network (probabilistic, pSC)			Sparse functional network (partial, pFC)			Ratio (pFC/pSC)			Coupling (correlation, pSC–pFC)		
Global property	HC	CP	*P* value	HC	CP	*P* value	HC	CP	*P* value	HC	CP	*P* value
Whole-brain network												
Global node strength	210.27 (17.42)	165.90 (18.65)	4.7×10^{-8}*	0.157 (0.004)	0.155 (0.003)	0.265	7.5×10^{-4} (7.0×10^{-5})	9.5×10^{-4} (1.1×10^{-4})	4.7×10^{-7}*			
Global efficiency	3.09 (0.11)	2.75 (0.13)	6.2×10^{-9}*	4.7×10^{-3} (1.9×10^{-4})	4.6×10^{-3} (1.4×10^{-4})	0.013*	1.5×10^{-3} (7.4×10^{-5})	1.7×10^{-3} (8.7×10^{-5})	5.8×10^{-5}*	0.209 (0.027)	0.186 (0.016)	0.007*
Local efficiency	2.69 (0.11)	2.45 (0.10)	2.5×10^{-7}*	5.0×10^{-4} (5.8×10^{-5})	4.6×10^{-4} (4.3×10^{-5})	0.036*	1.9×10^{-4} (2.3×10^{-5})	1.9×10^{-4} (1.7×10^{-5})	0.873			
Motor network												
Global node strength	58.57 (4.49)	55.30 (5.11)	0.057	0.125 (0.007)	0.122 (0.005)	0.102	0.002 (2.0×10^{-4})	0.002 (2.1×10^{-4})	0.358			
Global efficiency	4.00 (0.24)	3.85 (0.26)	0.095	7.0×10^{-3} (9.3×10^{-4})	6.0×10^{-3} (7.5×10^{-4})	0.003*	1.7×10^{-3} (2.5×10^{-4})	1.6×10^{-3} (1.8×10^{-4})	0.020*	0.235 (0.039)	0.179 (0.065)	0.004*
Local efficiency	3.81 (0.31)	3.61 (0.32)	0.083	3.8×10^{-3} (7.1×10^{-4})	3.0×10^{-3} (5.1×10^{-4})	0.002*	1.0×10^{-3} (2.2×10^{-4})	8.5×10^{-4} (1.8×10^{-4})	0.029*			
Dorsal visual stream network												
Global node strength	50.91 (3.03)	47.82 (3.41)	0.009*	0.132 (0.006)	0.135 (0.007)	0.127	2.6×10^{-3} (2.4×10^{-4})	2.8×10^{-3} (2.6×10^{-4})	0.009*			
Global efficiency	3.33 (0.13)	3.23 (0.14)	0.052	0.007 (0.001)	0.007 (0.001)	0.951	2.2×10^{-3} (2.6×10^{-4})	2.3×10^{-3} (3.4×10^{-4})	0.559	−0.023 (0.040)	−0.019 (0.038)	0.755
Local efficiency	3.23 (0.25)	3.30 (0.21)	0.425	2.9×10^{-3} (3.7×10^{-4})	3.2×10^{-3} (5.0×10^{-4})	0.019*	8.8×10^{-4} (1.1×10^{-4})	9.8×10^{-4} (1.6×10^{-4})	0.049*			
Ventral visual stream network												
Global node strength	37.59 (2.43)	35.75 (2.84)	0.051	0.137 (0.008)	0.139 (0.009)	0.528	3.7×10^{-3} (4.2×10^{-4})	3.9×10^{-3} (2.4×10^{-4})	0.077			
Global efficiency	3.27 (0.12)	3.20 (0.12)	0.094	0.009 (0.001)	0.009 (0.001)	0.706	0.003 (3.8×10^{-4})	0.003 (3.4×10^{-4})	0.467	0.057 (0.064)	0.041 (0.052)	0.441
Local efficiency	3.31 (0.20)	3.42 (0.19)	0.126	0.005 (0.001)	0.005 (0.001)	0.315	0.002 (3.3×10^{-4})	0.002 (3.0×10^{-4})	0.672			

Mean (standard deviation).
*Signficant group difference.

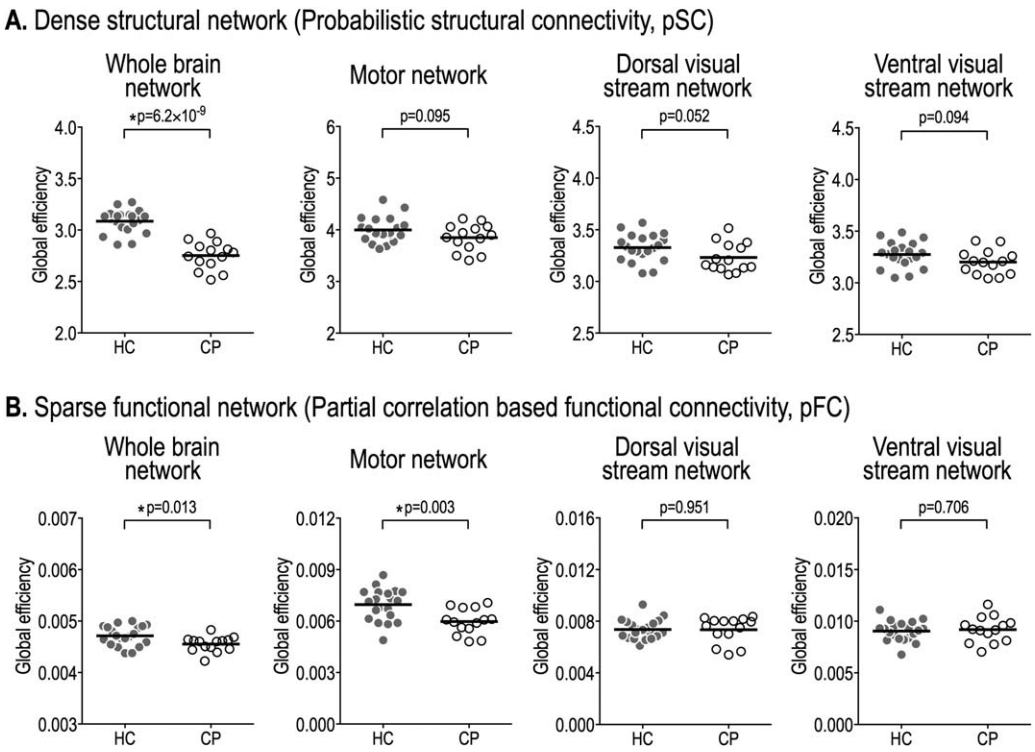

Figure 4.

Global efficiency of dense structural (pSC) and sparse functional networks (pFC) in the whole-brain, motor, and dorsal and ventral visual stream networks. Structural global efficiency of patients with cerebral palsy (CP) is significantly lower than that of healthy controls (HC) in the whole-brain network (A). However, there are no significant differences in the motor network (A). Functional network shows significantly reduced global efficiency of CP compared to HC in the whole-brain network and motor network (B).

networks in the whole-brain network and three specialized networks.

The structural network based on probabilistic connections showed significantly reduced global properties (global node strength and global efficiency) in the whole-brain network of patients with CP than those in healthy controls (Table II). Meanwhile, only the sparse functional networks and not the dense functional networks of CP showed reduced global and local efficiency compared to control subjects (Table II). Figures 4 and 5 summarize the group-wise differences in the global efficiency of sparse (partial correlation-based) functional networks, dense (probabilistic) structural networks, and their couplings in the whole-brain, motor, and two visual networks.

In the motor network, there were no statistical differences between the two groups for global network properties of dense (probabilistic) structural networks. However, the global and local efficiencies of the functional network derived from partial correlations were significantly lower in CP than healthy controls (global efficiency: $P = 0.003$, local efficiency: $P = 0.002$; Table II).

The global properties of the structural network in both the dorsal and ventral visual stream networks showed similar tendency and tended to be generally lower in patients with CP compared to healthy controls (Table II). However, these visual stream networks of CP showed increased global node strengths in functional networks, particularly in the dorsal stream network, compared to the healthy controls.

Global Efficiency Ratio of Functional Network to Structural Network

The ratios of global network properties of sparse functional networks to those of dense structural networks were summarized in Table II. The ratios of the global node strength and the global efficiency of sparse whole-brain functional networks to those of dense structural networks were significantly higher in CP patients compared to healthy controls (Fig. 5A and Table II). Meanwhile, in the motor network, the ratios of global and local efficiencies of sparse functional networks to those of dense structural networks were significantly lower in CP patients than in healthy controls. In the dorsal visual stream network, the ratios of global node strength and local efficiency were significantly higher in CP compared to healthy controls. No

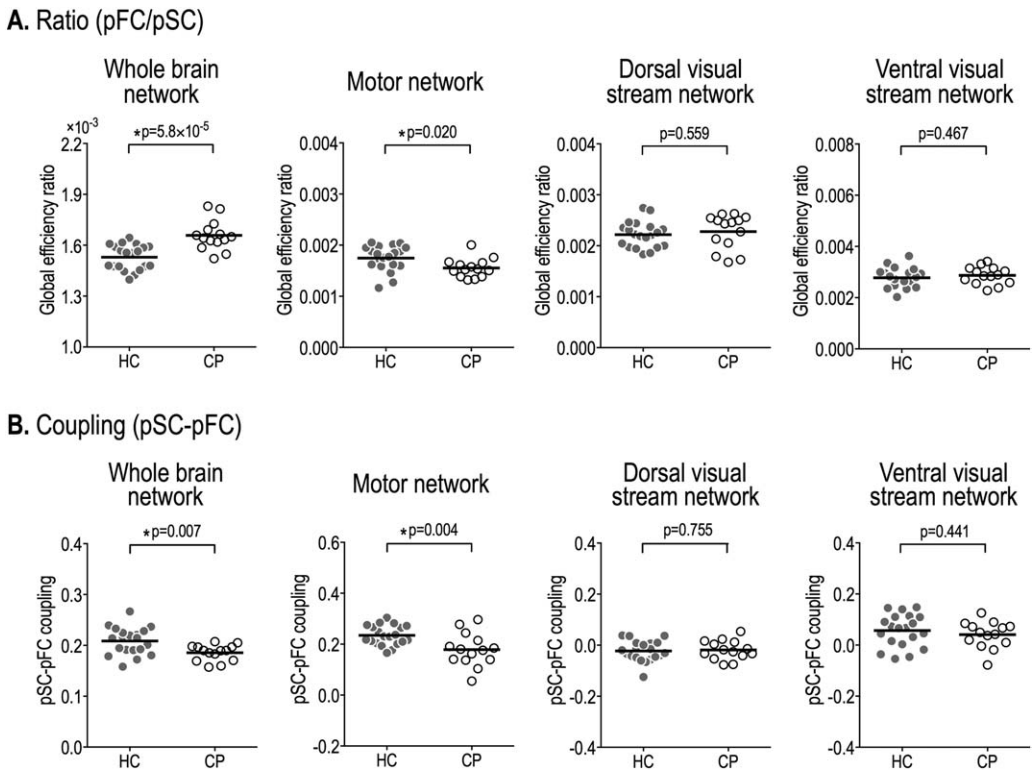

Figure 5.

Ratios of global efficiency of sparse functional network (pFC) to dense structural network (SC) and structural–functional network couplings in the whole-brain, motor, and dorsal and ventral visual stream networks. The ratio of the global efficiencies of whole-brain sparse functional network to dense structural network is significantly higher in cerebral palsy (CP) than healthy controls (HC), whereas the ratios of the motor network are significantly lower in CP compared to HC (A). Structure–function coupling (Pearson correlation coefficient) between a vectorized dense structural connectivity matrix and a sparse functional connectivity matrix was significantly reduced in CP at the whole-brain network and motor network, but not at the dorsal and ventral visual stream networks (B).

significant group-wise differences in the ratios of global network properties were found in the ventral visual stream network.

Couplings of Structural–Functional Networks

Structure–function network couplings—dense structural and sparse functional networks—in patients and controls are presented in Figure 5B and Table II. In the whole-brain network, patients with CP showed significantly lower structure–function network couplings compared to healthy controls when dense structural network was correlated with sparse functional network (two sample t tests, pSC–pFC: HC = 0.21 ± 0.03, CP = 0.19 ± 0.02, $P = 0.007$). The motor networks in CP patients also showed significantly reduced structure–function couplings (pSC–pFC: HC = 0.24 ± 0.04, CP = 0.18 ± 0.07, $P = 0.004$). We found that there were no significant group-wise differences in structure–function decoupling of the dorsal stream network and the visual stream network.

DISCUSSION

We investigated the brain networks in CP from the perspective of a structural and functional relationship; this is an important issue in understanding the brain, according to the reviews of Buckner et al. [2008], Honey et al. [2009], Van Dijk et al. [2010], and Park and Friston [2013]. Using graph-theoretical analysis of the structural–functional relationship, we found that functional networks embedded differently in the structural networks of patients with CP compared to healthy controls based on the network systems.

Consistent with the results of a previous study on preterm children with CP [Ceschin et al., 2015], patients with SDCP had significantly lower structural connections with other brain regions (node strength at each node) than healthy controls across the whole brain, except for the left motor cortical areas, left angular gyrus, bilateral orbitofrontal lobes, and anterior temporal lobes. The reduced global node strength (average node strength across the whole brain) and global efficiency (Table II) imply the inefficient structural network architecture for information exchange in CP.

Functional networks in the whole brain, however, did not behave in the same way as structural networks. Patients with SDCP showed intact functional interaction with other brain regions (global node strength) or slightly inferior capacity for information exchange (global efficiency) over the whole-brain network than healthy controls. Most brain regions maintained functional connection with other brain regions (node strength at each node) over reduced structural paths. Although the reduction in the global efficiency of partial correlation-based functional network passed the statistical significance test ($P = 0.013$), the amount of reduction was less prominent than in the structural network (Table II). This was obvious in the significantly increased function–structure ratios of global efficiency in CP compared to controls (Fig. 5A), which suggest less reduced (relatively enhanced) functional network information flow over the impaired structural networks. The intact functional network (specifically, in global node strength) over the altered structural network of the whole brain explains the decreased structure–function coupling, that is, increased deviation of the functional network from the structural network in CP patients compared to the control group (Table II).

In contrast to the whole-brain network, the motor network showed a different structure-function relationship, with relatively intact (or less deficient) structural but impaired functional network topologies. The left precentral and paracentral gyri of CP patients had intact structural node strengths compared to healthy controls (Fig. 3B). Indeed, the PVL location in CP does not highly overlap with the corticospinal tract, thalamocortical pathway, or pathways among regions in the motor network (Fig. 2B). Patients with CP also had relatively preserved global efficiency, local efficiency, and global node strength in the structural network of the motor network (Table II). However, patients had reduced global efficiency in the functional network, with a significantly reduced function–structure ratio. Deviation (or decoupling) of the functional network from the structural network was also found in the motor network of CP. Despite similar deviation found in the whole-brain network, the structure–function decoupling in the motor network of CP may be associated with reduced efficiency in the functional motor network. This result may support the network-theoretic explanation for the dominance of motor-related dysfunction in CP despite the widespread effects of prenatal injuries.

This structure–function alteration was relatively motor network-specific as the visual stream networks, particularly the ventral visual stream network, did not show divergence from the normal structure–function relationship found in the motor network. No significant intergroup differences were found in the structural and functional network properties and their relationships in the ventral visual stream network. The network properties (global node strength and global efficiency) of the dorsal stream network showed similar trends of group differences (patients vs healthy controls) with those of the ventral stream network, but there were more significant group differences. There was an increase in local efficiency of the functional network and in the functional–structural ratios of global node strength and local efficiency in the dorsal stream network of CP compared to healthy controls. These properties are part of the typical patterns of the whole brain network except for the normal decoupling between structural and functional networks in CP.

Although we evaluated two visual stream networks as reference points for evaluating exclusive changes in the motor system, the manifestations of motor impairment in CP may not be separable from the visual network, as these systems are interconnected with high complexity. In previous studies, patients with PVL had a relatively high incidence of cerebral visual impairment such as oculomotor disorders, low visual acuity, and reduced visual fields [Cioni et al., 1997], and high-level visual perception, related to deficits in the visuo-motor connectivity for eye movements and mental visual construction, requiring mental simulation of movement and transformation [Bottcher, 2010]. These faculties are more associated with the dorsal stream regions than the ventral stream regions [Milner, 2012; Schenk and McIntosh, 2010]. The prominent deficit in the dorsal stream regions may possibly be associated with PVL locations, which are closely positioned near the dorsal stream pathway as shown in Figure 2B. However, this study lacks data to provide a strong evidence for vision-specific alterations in the visual stream network topology that would be consistent with the previous studies, except for the observation that there was stronger deviation from healthy network properties in the dorsal visual stream network than in the ventral stream network. We may attribute these findings to the fact that recruited patients had mostly mild motor impairments (GMFCS levels 1 and 2). As we did not measure visual performance of patients that participated in this study, the conclusion for the relationship between visuo-motor behaviors and visual networks requires further study.

What caused different patterns of structure–function relationships in the whole brain and other subnetworks is still an open question. Previous studies have suggested that structural alterations in CP with PVL are rather widespread across the whole brain white matter [Ceschin et al., 2015; Englander et al., 2013; Lee et al., 2011b; Skranes et al., 2007]. Despite widespread structural alterations, the prevalence of cognitive impairment in CP is relatively less (23–44%), depending on the subtype of CP [Odding et al., 2006]. The relationship between the cognitive impairments and structural deficits in CP is not fully resolved [Fennell and Dikel, 2001]. We speculated that the brain systems responsible for cognitive functions in CP undergo functional reorganization over the structural network with altered pathways. This is partly evidenced by the intact functional node strengths over a damaged structural network.

As the brain has great ability to compensate for neuronal injury during the developmental period [Juenger et al., 2008;

Staudt, 2007], compensatory mechanisms might reduce wide-spread effects of prenatal insults during development, except in motor-related regions. Functional reorganization might be achieved by means of maintaining functional connectivity with other brain regions over the limited structural pathways. Although the biological basis of functional maintenance (or relative enhancement) over reduced structural connectivity might not be resolved in this study, we note that the functional connectivity is not only governed by extrinsic axonal projections (reflected in DTI tractography for the structural network construction), but also modulated by regional intrinsic or indirect factors such as changes in synaptic efficacy, neuromodulation, and/or polysynaptic connectivity [Park and Friston, 2013].

Similarly, impaired functional networks over intact (or less impaired) structural networks in the motor regions of CP can be explained by alterations in intraregional neuronal properties rather than inter-regional structural connectivity. As an evidence for intraregional alterations, previous studies using ^{18}F-fluoroflumazenil (^{18}F-FFMZ) positron emission tomography (PET) showed increased regional gamma-aminobutyric acid type A (GABA-A) receptor binding potential in the posterior and medial brain regions, including bilateral motor areas in children with SDCP [Lee et al., 2007, 2011b]. The increased GABA-A receptor binding potential in the local area may be associated with abnormal functional connectivity in other brain regions. Indeed, GABA-A distribution was also higher in the ipsilateral motor-related brain areas of patients with hemiplegic CP, but demonstrated reduced functional connectivity [Park et al., 2013b].

However, we cannot disregard the possibility of reorganization in the structural white matter pathways in the motor network. For example, Lee et al. [2011b] showed a significant positive correlation between symptom severity (GMFCS score) and fractional anisotropy of diffusion tensor imaging in the corticospinal tract (white matter in motor cortical areas), while there was a negative correlation in most other brain regions. This suggests that patients with severe symptoms have increased structural connectivity in the white matter near the primary motor areas or corticospinal tracts. This positive correlation may explain the relatively intact global efficiency in the structural network of the motor systems, despite the severe reduction in functional network efficiency, possibly due to intraregional factors explained above. To better understand the underlying mechanism affecting the motor cortex in CP, further studies would be necessary.

Besides the neurobiological findings of CP networks, this study also suggests the importance of a network-centric perspective of the brain disorders. We found reduced node strengths in most structural network brain areas. As the node strength is the sum of fiber counts that interconnect with all the other brains, structural alteration may exist not simply in a single edge level, but in a multitude of edges and thus can be sensitively detected using a multivariate approach like node strength.

Our main finding in the functional motor network of CP was an altered network topology over an alteration in the single edges (interaction between two nodes). As discussed by Park and Friston [2013], a network is not a simple combination of individual pathways, but rather, a systematic organization of interactions within the network. Thus, an altered corticospinal pathway or thalamocortical pathway found in previous studies on CP [Arzoumanian et al., 2003; Lee et al., 2011b; Pannek et al., 2014; Scheck et al., 2012; Thomas et al., 2005] or altered functional connectivity in CP [Dinomais et al., 2012; Lee et al., 2011a; Papadelis et al., 2014] may not be sufficient enough to explain the topological architecture of the motor-related brain regions, including cortical and subcortical regions. What is more important might be the nature of circuits and a combination of edges [Marder, 2012].

In the construction of structural and functional networks, one should carefully consider "dense" versus "sparse" connections. Variations in structural connectivity metrics can affect the characterization of structural connections between different regions [Khalsa et al., 2014]. Probabilistic tractography accounts for the uncertainty of local fiber orientations or distributed connectivity [Craddock et al., 2013]. Thus, structural connections derived from deterministic tractography tend to be sparser than those measured by probabilistic tractography [Bonilha et al., 2015]. As measures of functional connectivity, we used partial correlation in constructing sparse functional brain networks. We also evaluated dense functional networks using Pearson-correlation, but we did not find a significant difference in the structure–function coupling between the groups (Supporting Information). Pearson correlation method cannot factor out the latent effects of a third and/or a fourth node that may modulate between the two nodes. This makes interpretation of the correlative activities unclear, whether they are from intrinsic structural connections or from polysynaptic inductions, common modulatory effects, or common feed-forward projections via the thalamus [van den Heuvel et al., 2009]. On the contrary, partial correlation was more efficient in revealing direct associations between the brain areas. In this study, partial correlation showed good sensitivity in detecting structural and functional differences in the global network efficiency and structure–function coupling between the groups. In consistent with the current result, partial correlation is known to be closer to structural brain network than Pearson correlation [Marrelec et al., 2006; Smith et al., 2011].

This study had several limitations. We could not correlate structure–function relationships with motor performances owing to small samples of narrowly distributed motor symptom scales (mostly GMFCS 1), and with individual cognitive performances owing to the lack of behavioural measures. As healthy controls were gathered from different studies, no consistent measures of cognitive function other than age and gender could be used. The situation was similar for the patients except that consistent motor scores and birth-related information, essential for researches about movement disorders, were

gathered. Thus, the association between structure–function relationships and well-documented cognitions remains to be discovered. We do not disregard the possibility of errors in the network construction methods, such as missing fibers due to limitations of DTI, artifacts in fMRI, and in the definition of network nodes. Although each processing step was controlled carefully by visual analysis and use of in-house software, the technical challenges remain for further advancement of data acquisition and analysis methods. Multivariate graph-theoretical measures used in this study may mitigate the estimation errors inherent with single connectivity estimation. In the graph theory of the human connectome, measures for network properties are initially developed on the structural network. However, we believe that the same measures are also meaningful on the functional network as an index for efficiency of information flow over the structural network.

In summary, we investigated brain networks in SDCP with PVL from the perspective of the relationship between structure and function. We found severely altered structural networks, but improved (or less severe) information exchange (functional network) among regions in the whole brain, suggesting reorganization. Meanwhile, the motor network in CP showed highly impaired information exchange over intact pathways. This result is clearly detected in partial-correlation-based functional networks. This study suggests that graph theoretic approach is advantageous in describing the neurobiology of brain disorder and that the structure–function relationship plays an important role in understanding CP.

ACKNOWLEDGMENT

This work was supported by the National Research Foundation of Korea (NRF) grant funded by the Korea government(MSIP) (No. 2014R1A2A1A10052762). The authors thank Ms. Hanseul Choi for her help in manuscript editing.

REFERENCES

Arzoumanian Y, Mirmiran M, Barnes PD, Woolley K, Ariagno RL, Moseley ME, Fleisher BE, Atlas SW (2003): Diffusion tensor brain imaging findings at term-equivalent age may predict neurologic abnormalities in low birth weight preterm infants. AJNR Am J Neuroradiol 24:1646–1653.

Ashburner J (2007): A fast diffeomorphic image registration algorithm. NeuroImage 38:95–113.

Behrens TE, Berg HJ, Jbabdi S, Rushworth MF, Woolrich MW (2007): Probabilistic diffusion tractography with multiple fibre orientations: What can we gain? NeuroImage 34:144–155.

Bonilha L, Gleichgerrcht E, Fridriksson J, Rorden C, Breedlove JL, Nesland T, Paulus W, Helms G, Focke NK (2015): Reproducibility of the structural brain connectome derived from diffusion tensor imaging. PLoS One 10:e0135247.

Bottcher L (2010): Children with spastic cerebral palsy, their cognitive functioning, and social participation: A review. Child. Neuropsychology 16:209–228.

Buckner RL, Andrews-Hanna JR, Schacter DL (2008): The brain's default network: Anatomy, function, and relevance to disease. Ann N Y Acad Sci 1124:1–38.

Bullmore E, Sporns O (2009): Complex brain networks: Graph theoretical analysis of structural and functional systems. Nat Rev Neurosci 10:186–198.

Burton H, Dixit S, Litkowski P, Wingert JR (2009): Functional connectivity for somatosensory and motor cortex in spastic diplegia. Somatosens Mot Res 26:90–104.

Ceschin R, Lee VK, Schmithorst V, Panigrahy A (2015): Regional vulnerability of longitudinal cortical association connectivity: Associated with structural network topology alterations in preterm children with cerebral palsy. NeuroImage Clin 9: 322–337.

Cioni G, Fazzi B, Coluccini M, Bartalena L, Boldrini A, van Hof-van Duin J (1997): Cerebral visual impairment in preterm infants with periventricular leukomalacia. Pediatr Neurol 17: 331–338.

Cocchi L, Harding IH, Lord A, Pantelis C, Yucel M, Zalesky A (2014): Disruption of structure-function coupling in the schizophrenia connectome. NeuroImage Clin 4:779–787.

Craddock RC, Jbabdi S, Yan CG, Vogelstein JT, Castellanos FX, Di Martino A, Kelly C, Heberlein K, Colcombe S, Milham MP (2013): Imaging human connectomes at the macroscale. Nat Methods 10:524–539.

Deco G, Jirsa VK, McIntosh AR (2011): Emerging concepts for the dynamical organization of resting-state activity in the brain. Nat Rev Neurosci 12:43–56.

Dempster AP (1972): Covariance selection. Biometrics Biometrics 28:157–175.

Dinomais M, Groeschel S, Staudt M, Krageloh-Mann I, Wilke M (2012): Relationship between functional connectivity and sensory impairment: Red flag or red herring? Hum Brain Mapp 33:628–638.

Englander ZA, Pizoli CE, Batrachenko A, Sun J, Worley G, Mikati MA, Kurtzberg J, Song AW (2013): Diffuse reduction of white matter connectivity in cerebral palsy with specific vulnerability of long range fiber tracts. NeuroImage Clin 2:440–447.

Fennell EB, Dikel TN (2001): Cognitive and neuropsychological functioning in children with cerebral palsy. J Child Neurol 16: 58–63.

Friedman J, Hastie T, Tibshirani R (2008): Sparse inverse covariance estimation with the graphical lasso. Biostatistics 9:432–441.

Friston K, Holmes A, Worsley K, Poline J, Frith C, Frackowiak R (1995): Statistical parametric maps in functional imaging: A general linear approach. Hum Brain Mapp 2:189–210.

Goodale MA, Ingle DJ, Mansfield RJ (1982): Analysis of Visual Behavior. MIT Press. pp 263–299.

Goodale MA, Milner AD (1992): Separate visual pathways for perception and action. Trends Neurosci 15:20–25.

Honey CJ, Sporns O, Cammoun L, Gigandet X, Thiran JP, Meuli R, Hagmann P (2009): Predicting human resting-state functional connectivity from structural connectivity. Proc Natl Acad Sci USA 106:2035–2040.

Huang S, Li J, Sun L, Ye J, Fleisher A, Wu T, Chen K, Reiman E, Alzheimer's Disease NeuroImaging I (2010): Learning brain connectivity of Alzheimer's disease by sparse inverse covariance estimation. NeuroImage 50:935–949.

Juenger H, Grodd W, Krageloh-Mann I, Staudt M (2008): (Re-)organization of basal ganglia in congenital hemiparesis with ipsilateral cortico-spinal projections. Neuropediatrics 39: 252–258.

Kahan J, Urner M, Moran R, Flandin G, Marreiros A, Mancini L, White M, Thornton J, Yousry T, Zrinzo L, Hariz M, Limousin P, Friston K, Foltynie T (2014): Resting state functional MRI in Parkinson's disease: The impact of deep brain stimulation on 'effective' connectivity. Brain J Neurol 137:1130–1144.

Keogh JM, Badawi N (2006): The origins of cerebral palsy. Curr Opin Neurol 19:129–134.

Khalsa S, Mayhew SD, Chechlacz M, Bagary M, Bagshaw AP (2014): The structural and functional connectivity of the posterior cingulate cortex: Comparison between deterministic and probabilistic tractography for the investigation of structure-function relationships. NeuroImage 102 Pt 1:118–127.

Latora V, Marchiori M (2001): Efficient behavior of small-world networks. Phys Rev Lett 87:198701.

Lee D, Park B, Jang C, Park HJ (2011a): Decoding brain states using functional magnetic resonance imaging. Biomed Eng Lett 2011:82–88.

Lee JD, Park HJ, Park ES, Kim DG, Rha DW, Kim EY, Kim DI, Kim JJ, Yun M, Ryu YH, Lee J, Jeong JM, Lee DS, Lee MC, Park CI (2007): Assessment of regional GABA(A) receptor binding using 18F-fluoroflumazenil positron emission tomography in spastic type cerebral palsy. NeuroImage 34: 19–25.

Lee JD, Park HJ, Park ES, Oh MK, Park B, Rha DW, Cho SR, Kim EY, Park JY, Kim CH, Kim DG, Park CI (2011b): Motor pathway injury in patients with periventricular leucomalacia and spastic diplegia. Brain 134:1199–1210.

Liu H, Roeder K, Wasserman L (2010): Stability approach to regularization selection (StARS) for high dimensional graphical models. Adv Neural Inf Process Syst 24:1432–1440.

Marder E (2012): Neuromodulation of neuronal circuits: Back to the future. Neuron 76:1–11.

Marrelec G, Krainik A, Duffau H, Pelegrini-Issac M, Lehericy S, Doyon J, Benali H (2006): Partial correlation for functional brain interactivity investigation in functional MRI. NeuroImage 32:228–237.

Milner AD (2012): Is visual processing in the dorsal stream accessible to consciousness? Proc Biol Sci 279:2289–2298.

Milner AD, Goodale MA (2006): The Visual Brain in Action. Oxford University Press.

Msall ME (2004): Developmental vulnerability and resilience in extremely preterm infants. JAMA J Am Med Assoc 292: 2399–2401.

Msall ME (2006): Complexity of the cerebral palsy syndromes: Toward a developmental neuroscience approach. JAMA 296: 1650–1652.

Nagae LM, Hoon AH, Jr., Stashinko E, Lin D, Zhang W, Levey E, Wakana S, Jiang H, Leite CC, Lucato LT, van Zijl PC, Johnston MV, Mori S (2007): Diffusion tensor imaging in children with periventricular leukomalacia: Variability of injuries to white matter tracts. AJNR Am J Neuroradiol 28:1213–1222.

Nam H, Park HJ (2011): Distortion correction of high b-valued and high angular resolution diffusion images using iterative simulated images. NeuroImage 57:968–978.

Odding E, Roebroeck ME, Stam HJ (2006): The epidemiology of cerebral palsy: Incidence, impairments and risk factors. Disabil Rehabil 28:183–191.

Pannek K, Boyd RN, Fiori S, Guzzetta A, Rose SE (2014): Assessment of the structural brain network reveals altered connectivity in children with unilateral cerebral palsy due to periventricular white matter lesions. NeuroImage Clin 5: 84–92.

Papadelis C, Ahtam B, Nazarova M, Nimec D, Snyder B, Grant PE, Okada Y (2014): Cortical somatosensory reorganization in children with spastic cerebral palsy: A multimodal neuroimaging study. Front Hum Neurosci 8:725.

Park B, Ko JH, Lee JD, Park HJ (2013a): Evaluation of node-inhomogeneity effects on the functional brain network properties using an anatomy-constrained hierarchical brain parcellation. PLoS One 8:e74935.

Park HJ, Friston K (2013): Structural and functional brain networks: From connections to cognition. Science 342:1238411.

Park HJ, Kim CH, Park ES, Park B, Oh SR, Oh MK, Park CI, Lee JD (2013b): Increased GABA-A receptor binding and reduced connectivity at the motor cortex in children with hemiplegic cerebral palsy: A multimodal investigation using 18F-fluoroflumazenil PET, immunohistochemistry, and MR imaging. J Nuclear Med 54:1263–1269.

Rubinov M, Sporns O (2010): Complex network measures of brain connectivity: Uses and interpretations. NeuroImage 52: 1059–1069.

Scheck SM, Boyd RN, Rose SE (2012): New insights into the pathology of white matter tracts in cerebral palsy from diffusion magnetic resonance imaging: A systematic review. Dev Med Child Neurol 54:684–696.

Schenk T, McIntosh RD (2010): Do we have independent visual streams for perception and action? Cogn Neurosci 1:52–62.

Schmidt R, Verstraete E, de Reus MA, Veldink JH, van den Berg LH, van den Heuvel MP (2014): Correlation between structural and functional connectivity impairment in amyotrophic lateral sclerosis. Hum Brain Mapp 35:4386–4395.

Skranes J, Vangberg TR, Kulseng S, Indredavik MS, Evensen KA, Martinussen M, Dale AM, Haraldseth O, Brubakk AM (2007): Clinical findings and white matter abnormalities seen on diffusion tensor imaging in adolescents with very low birth weight. Brain 130:654–666.

Skudlarski P, Jagannathan K, Calhoun VD, Hampson M, Skudlarska BA, Pearlson G (2008): Measuring brain connectivity: Diffusion tensor imaging validates resting state temporal correlations. NeuroImage 43:554–561.

Smith SM, Miller KL, Salimi-Khorshidi G, Webster M, Beckmann CF, Nichols TE, Ramsey JD, Woolrich MW (2011): Network modelling methods for fMRI. NeuroImage 54: 875–891.

Staudt M (2007): (Re-)organization of the developing human brain following periventricular white matter lesions. Neurosci Biobehav Rev 31:1150–1156.

Taniwaki T, Okayama A, Yoshiura T, Nakamura Y, Goto Y, Kira J, Tobimatsu S (2003): Reappraisal of the motor role of basal ganglia: A functional magnetic resonance image study. J Neurosci 23:3432–3438.

Thomas B, Eyssen M, Peeters R, Molenaers G, Van Hecke P, De Cock P, Sunaert S (2005): Quantitative diffusion tensor imaging in cerebral palsy due to periventricular white matter injury. Brain 128:2562–2577.

Tzourio-Mazoyer N, Landeau B, Papathanassiou D, Crivello F, Etard O, Delcroix N, Mazoyer B, Joliot M (2002): Automated anatomical labeling of activations in SPM using a macroscopic anatomical parcellation of the MNI MRI single-subject brain. NeuroImage 15:273–289.

van den Heuvel MP, Mandl RC, Kahn RS, Hulshoff Pol HE (2009): Functionally linked resting-state networks reflect the underlying structural connectivity architecture of the human brain. Hum Brain Mapp 30:3127–3141.

van den Heuvel MP, Sporns O, Collin G, Scheewe T, Mandl RC, Cahn W, Goni J, Hulshoff Pol HE, Kahn RS (2013): Abnormal rich club organization and functional brain dynamics in schizophrenia. JAMA Psychiatry 70:783–792.

Van Dijk KR, Hedden T, Venkataraman A, Evans KC, Lazar SW, Buckner RL (2010): Intrinsic functional connectivity as a tool for human connectomics: Theory, properties, and optimization. J Neurophysiol 103:297–321.

Wang J, Zhou T, Qiu M, Du A, Cai K, Wang Z, Zhou C, Meng M, Zhuo Y, Fan S, Chen L (1999): Relationship between ventral stream for object vision and dorsal stream for spatial vision: An fMRI + ERP study. Hum Brain Mapp 8:170–181.

Wei L, Zhang J, Long Z, Wu GR, Hu X, Zhang Y, Wang J (2014): Reduced topological efficiency in cortical-basal Ganglia motor network of Parkinson's disease: A resting state fMRI study. PLoS One 9:e108124.

Zou N, Chetelat G, Baydogan MG, Li J, Fischer FU, Titov D, Dukart J, Fellgiebel A, Schreckenberger M, Yakushev I (2015): Metabolic connectivity as index of verbal working memory. J Cereb Blood Flow Metab 35:1122–1126.